

A new white light emitting nanophosphor

Shaath SKK^{1,2}, Swart HC¹ and Ntwaeaborwa OM^{1,*}

¹ Department of Physics, University of the Free State, Bloemfontein, ZA9300, South Africa.

² Department of Physics, Islamic University, P. O. Box 108, Gaza, Palestine.

* Corresponding author: ntwaeab@ufs.ac.za

Abstract. White light was produced from CaAl₂O₄ nanophosphor co-doped with Tb³⁺ and Eu³⁺. The short time and low temperature reaction combustion route was used to synthesize CaAl₂O₄:Tb³⁺,Eu³⁺ nanophosphors using metal nitrates precursors and urea as fuel. The crystalline structure and particle morphology were determined using X-ray diffraction and Scanning electron microscopy, respectively. The optical properties were studied by photoluminescence (PL) spectroscopy and the UV-Vis spectrometer in the range 800-200 nm. The excitation spectra were recorded by monitoring the three main emissions, namely blue at 438 nm, green at 543 nm and red at 617 nm. 227 nm was found to be the most suitable excitation wavelength to generate, simultaneously, blue and green emission from Tb³⁺ and red emission from Eu³⁺ whose combination constituted white light. The blue and green were respectively attributed to the 4f-4f transitions of Tb³⁺ by ⁵D₃→⁷F_J (J= 6-2) and ⁵D₄→⁷F_J (J = 0-6) while the red emission was attributed to ⁵D₀→⁷F_J (J=0-4) transitions of Eu³⁺. Preliminary results on the structure and PL properties of this phosphor are reported.

1. Introduction

Scientists and researchers are conducting research in search for suitable host lattices that can be used to prepare phosphors for solid state lighting. The host must, among other things, be chemically and thermally stable. Alkali earth aluminates with a general formula MA₂O₄ (M = Ba, Ca or Sr) are widely used as hosts for trivalent rare-earth (Dy³⁺, Nd³⁺, etc) and divalent europium (Eu²⁺) ions for the preparation of light emitting materials (phosphors) with persistent luminescence. Aluminates are more chemically stable, environmentally friendly [1] and they can be easily produced cost-effectively. Therefore the study of the preparation and characterization of aluminates based phosphors is growing rapidly. Phosphors such as SrAl₂O₄:Eu²⁺, CaAl₂O₄:Eu²⁺ and BaAl₂O₄:Eu²⁺ phosphors, co-activated with different rare-earths (Dy³⁺, Nd³⁺, Pr³⁺) have been reported [2]. These phosphors are usually produced cost-effectively, at relatively low temperature and a short reaction time by the combustion method using metal nitrates as starting materials and urea as a fuel. White light in many practical applications is generated by combining currently three available colours blue, green and red phosphor in appropriate ratios. For example, in traditional white light emitting diodes (LEDs), white light is generated by combining a InGaN-based blue diode with a yellow phosphor such as YAG:Ce³⁺ or by combining a UV chip with a three converter system of red, green and blue phosphors. Furthermore, white light from fluorescent lamps is produced from combining tri-colour phosphors which emit blue, green and red light upon excitation by ultraviolet radiation. Shaath et al, [3] produced white light from Ca_xSr_(1-x)Al₂O₄:Tb³⁺,Eu³⁺ nanocrystalline phosphor for application in solid state lighting devices such as fluorescent lamps and LEDs. In this study, a potential white light emitting nanocrystalline phosphor was prepared by co-doping terbium (Tb³⁺) and europium (Eu³⁺) in a calcium aluminate (CaAl₂O₄) host.

2. Experimental

2.1 Sample Preparation

A combustion method was used to prepare Tb³⁺ and Eu³⁺ single and co-doped CaAl₂O₄ nanophosphor. The metal nitrates of Ca(NO₃)₂.4H₂O, Al(NO₃)₃.9H₂O, Tb(NO₃)₃.5H₂O, Eu(NO₃)₃.5H₂O and urea

$\text{CO}(\text{NH}_2)_2$ of AR grade purchased from Merck, South Africa were used as starting materials (precursors) and were used as obtained without further purification. The distilled water used to dissolve the precursors with vigorous stirring at 50°C for 0.3 hr until the solution became clear. The resulting solution was transferred to a muffle furnace maintained at $450 \pm 10\%$ °C. The transparent solution started to boil and undergo dehydration, followed by decomposition and escaping large amounts of gases (nitrogen, ammonia and oxides of carbon). White foamy and voluminous ash was produced after spontaneous ignition occurred and underwent smouldering combustion with enormous swelling. The combustion reaction was completed in ~ 5 minutes. The product was cooled to room temperature and the ashes were ground gently into fine powders. The powders were characterized without any further post-preparation treatment.

2.2 Experimental Techniques

The crystalline structure of $\text{CaAl}_2\text{O}_4:\text{Tb}^{3+};\text{Eu}^{3+}$ was analysed by Bruker D8 ADVANCE powder diffractometer with $\text{Cu K}\alpha$ radiation, $\lambda=1.5406\text{\AA}$. The optical properties were characterized by UV-Vis spectroscopy Lambda 950 and the Varian Cary Eclipse fluorescence spectrophotometer. PL (excitation and emission) were measured for different samples $\text{CaAl}_2\text{O}_4:\text{Tb}^{3+}$, $\text{CaAl}_2\text{O}_4:\text{Eu}^{3+}$ and $\text{CaAl}_2\text{O}_4:\text{Tb}^{3+};\text{Eu}^{3+}$ with different excitation wavelengths. All measurements were carried out at room temperature and atmospheric pressure.

3. Analysis and results discussion

3.1. XRD Study

Figure 1 shows the X-ray diffraction (XRD) patterns of $\text{CaAl}_2\text{O}_4:\text{Tb}^{3+};\text{Eu}^{3+}$ nanophosphor. The patterns correspond to the standard monoclinic structure of CaAl_2O_4 in JCPDS file No. 70-0134. The diffraction peak at $2\theta=25.34^\circ$ was indexed as the (012) peak of Al_2O_3 [4] which was possibly formed during an unwanted reaction between Al^{3+} and O^{2-} from the precursors. The Debye-Scherrer relation was used to estimate the average particle size for the (220) diffraction peak and was found to be ~ 16 nm. The calculated lattice parameters are ($a = 8.71 \text{ \AA}$, $b = 8.084 \text{ \AA}$, $c = 15.23 \text{ \AA}$ with α and $\gamma = 90^\circ$ but $\beta = 90.45^\circ$) which are in a good agreement with the standard monoclinic CaAl_2O_4 referenced in JCPDS file No. 70-0134 ($a = 8.700 \text{ \AA}$, $b = 8.092 \text{ \AA}$, $c = 15.19 \text{ \AA}$ with α and $\gamma = 90^\circ$ but $\beta = 90.17^\circ$).

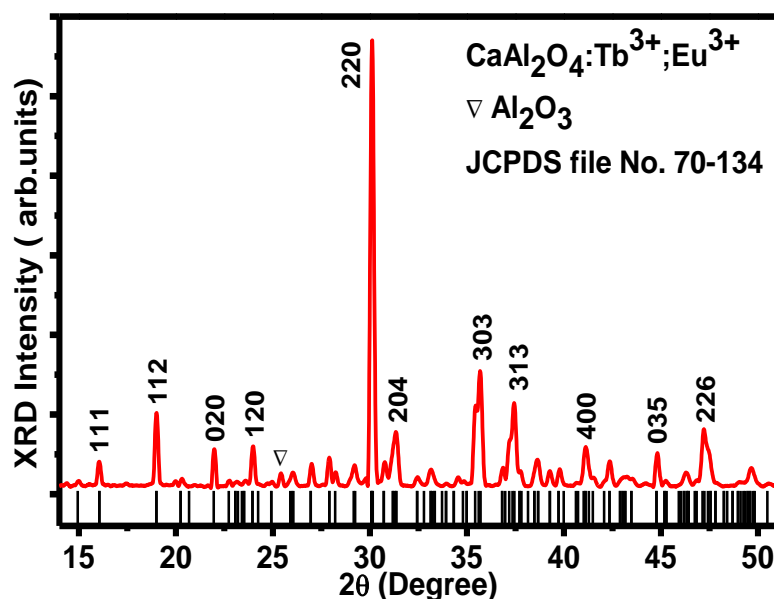
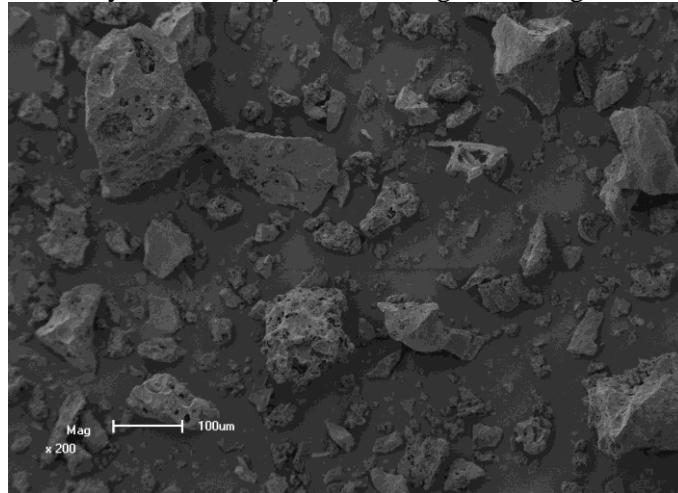


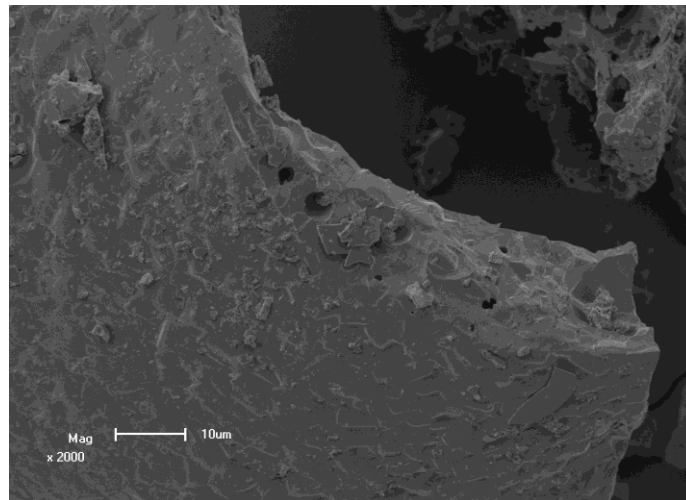
Figure 1. XRD spectrum of $\text{CaAl}_2\text{O}_4:\text{Tb}^{3+};\text{Eu}^{3+}$ nanophosphors.

3.2. SEM micrograph study

Figure 2(a-b) show the SEM micrograph images of the as-prepared monoclinic $\text{CaAl}_2\text{O}_4:\text{Tb}^{3+};\text{Eu}^{3+}$ nanophosphor with two different magnifications. The foamy and agglomerate particle nature of the powder is clear in figure 2(a-b). The foamy structure of $\text{CaAl}_2\text{O}_4:\text{Tb}^{3+};\text{Eu}^{3+}$ reflects the inherent nature of the combustion process. Figure 2 (a-b) shows an irregular shape with a lot of voids and pores of the surface of the powder, which may be formed by the evolved gases during combustion reaction.



(a)



(b)

Figure 2(a-b). SEM micrograph images of the $\text{CaAl}_2\text{O}_4:\text{Tb}^{3+};\text{Eu}^{3+}$ nanophosphor.

3.3 UV-Vis study

Figure 3 shows the diffuse reflectance spectrum of the $\text{CaAl}_2\text{O}_4:\text{Tb}^{3+};\text{Eu}^{3+}$ nanophosphor. Two absorption peaks at 213 nm and at 330 nm were observed. The absorption peak observed at 213 nm is attributed to the interband transition of CaAl_2O_4 . [5] The absorption peak near 330 nm was assigned to the $\text{O}^{2-}-\text{Eu}^{3+}$ charge transfer band [6]. The band gap energy of the $\text{CaAl}_2\text{O}_4:\text{Tb}^{3+};\text{Eu}^{3+}$ was estimated from a plot of $(\alpha E)^2$ versus photon energy E shown in figure 4. The band gap energy was estimated from the linear part of the straight line to the $(\alpha E)^2 = 0$ axis and by extrapolating was found to be $5.3 \pm 0.1 \text{ eV}$. This result is close to the value of 5.78 reported in ref. [7].

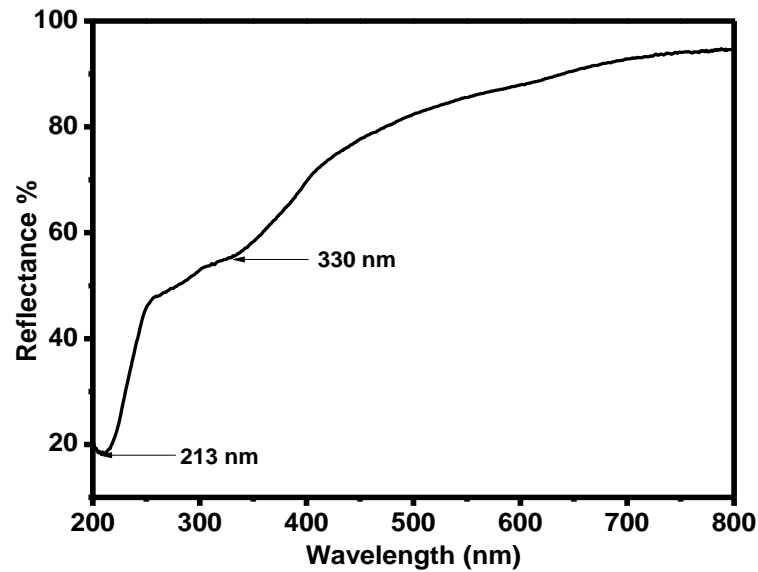


Figure 3. Diffuse reflectance spectrum of the $\text{CaAl}_2\text{O}_4:\text{Tb}^{3+};\text{Eu}^{3+}$ nanophosphor.

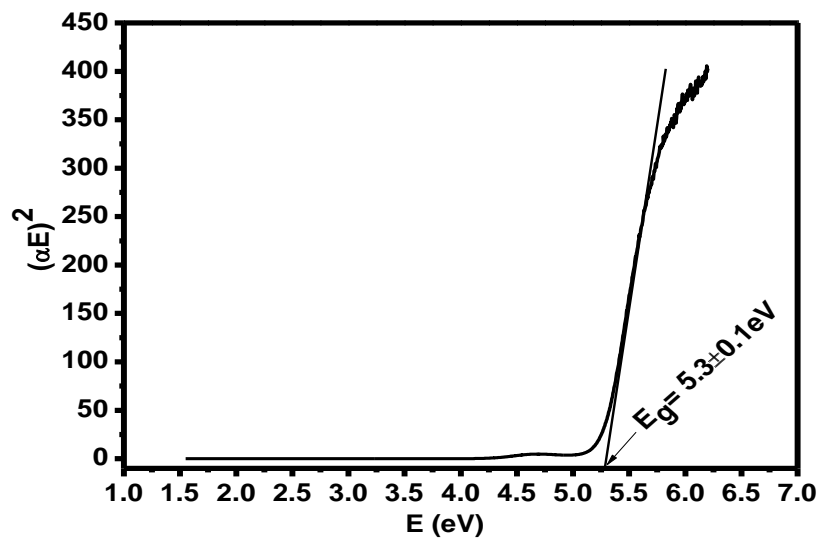


Figure 4. Plots of $(\alpha h\nu)^2$ versus photon energy ($h\nu$) to determine the band gap energy of the $\text{CaAl}_2\text{O}_4:\text{Tb}^{3+};\text{Eu}^{3+}$ nanophosphor.

3.3. Photoluminescence study

Photoluminescence (PL) excitation spectrum of $\text{CaAl}_2\text{O}_4:\text{Tb}^{3+};\text{Eu}^{3+}$ nanophosphor is shown in figure 5. The excitation spectra were recorded for three different emissions at 437 and 543 nm from Tb^{3+} and 617 nm from Eu^{3+} . There are two major peaks located at 227 and 237 nm due to direct excitation of Tb^{3+} and are assigned to the $4f \rightarrow 5d$ transitions [8,9]. The excitation peak at ~ 240 nm are due to $\text{Eu}^{3+} \rightarrow \text{O}^{2-}$ charge transfer transitions resulting from transfer of electrons from O^{2-} ($2p^6$) orbitals to the $4f^7$ and $4f^6$ states [10].

The PL emission spectrum of the $\text{CaAl}_2\text{O}_4:\text{Tb}^{3+};\text{Eu}^{3+}$ nanophosphor observed when exciting the phosphor at 227 nm is shown in figure 6. The PL emission spectra of Tb^{3+} and Eu^{3+} single doped CaAl_2O_4 also were recorded when exciting the phosphors at 227 nm are shown in the insets. The PL emission spectra of $\text{CaAl}_2\text{O}_4:\text{Tb}^{3+}$ consists of major green emission at 543 nm due to the ${}^5\text{D}_4 \rightarrow {}^7\text{F}_5$ transitions of Tb^{3+} and minor emissions at 380 nm (violet), 416 nm (blue), and 437 nm (blue) due to the ${}^5\text{D}_3 \rightarrow {}^7\text{F}_J$ ($J = 6,5,4$) transitions of Tb^{3+} . The PL emission spectrum of the $\text{CaAl}_2\text{O}_4:\text{Eu}^{3+}$ in the

other inset consist of major red emission at 617 nm due to the ${}^5D_0 \rightarrow {}^7F_2$ electric dipole transitions of Eu^{3+} and minor emission at 593 nm due to magnetic dipole transitions of Eu^{3+} [11]. The PL emission spectrum of the $\text{CaAl}_2\text{O}_4:\text{Tb}^{3+},\text{Eu}^{3+}$ nanophosphor exhibits white light which is a result of simultaneous emissions of blue and green light from Tb^{3+} , and red light from Eu^{3+} .

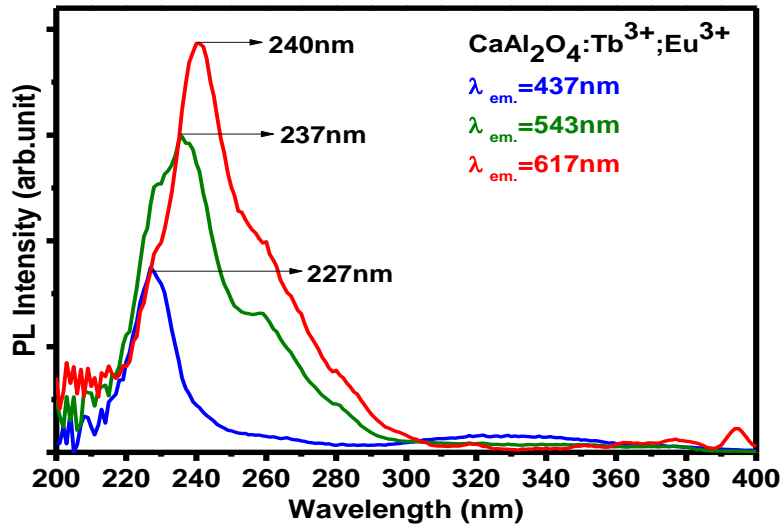


Figure 5: PL excitation spectra of $\text{CaAl}_2\text{O}_4:\text{Tb}^{3+},\text{Eu}^{3+}$ nanophosphor.

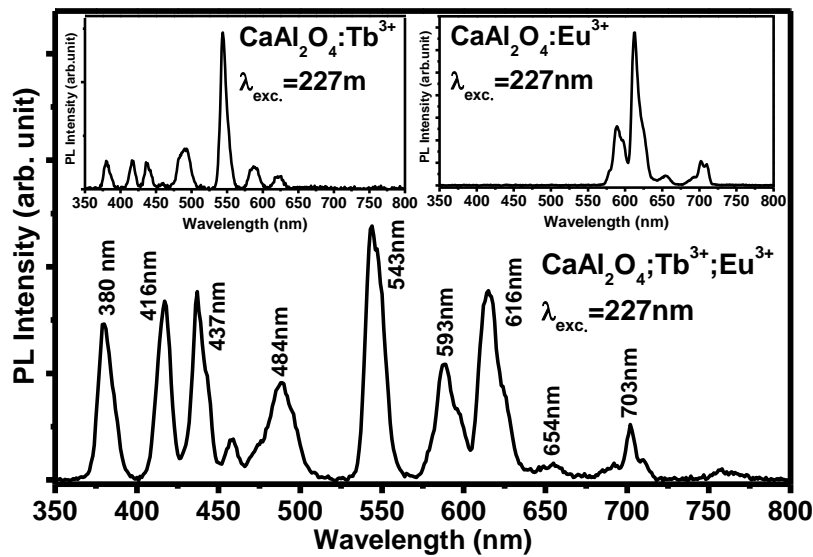


Figure 6: PL emission spectrum of $\text{CaAl}_2\text{O}_4:\text{Tb}^{3+},\text{Eu}^{3+}$ nanophosphor and the two insets are the PL emission spectra of $\text{CaAl}_2\text{O}_4:\text{Tb}^{3+}$ and $\text{CaAl}_2\text{O}_4:\text{Eu}^{3+}$. All were excited at 227 nm.

Figure 7 depicts the CIE diagram and the chromaticity coordinates for the $\text{CaAl}_2\text{O}_4:\text{Tb}^{3+}$, $\text{CaAl}_2\text{O}_4:\text{Eu}^{3+}$ and $\text{CaAl}_2\text{O}_4:\text{Tb}^{3+},\text{Eu}^{3+}$. The calculated chromaticity coordinates for the white light emitted from $\text{CaAl}_2\text{O}_4:\text{Tb}^{3+},\text{Eu}^{3+}$ nanophosphor are given by $(x = 0.354, y = 0.337)$, which is in agreement with the chromaticity coordinates of standard white light $(x = 0.333, y = 0.333)$ [12]. Also shown in the figure are the chromaticity coordinates of the red $\text{CaAl}_2\text{O}_4:\text{Eu}^{3+}$ given by $(x = 0.637, y = 0.360)$ and the green $\text{CaAl}_2\text{O}_4:\text{Tb}^{3+}$ given by $(x = 0.286, y = 0.477)$.

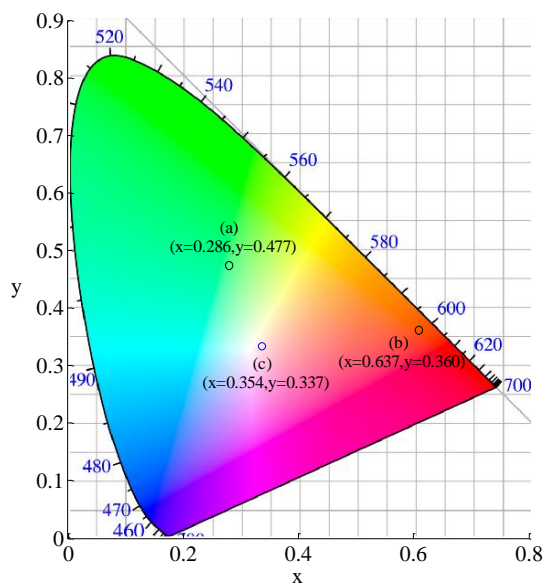


Figure 7: The CIE diagram and the chromaticity coordinates of (a) $\text{CaAl}_2\text{O}_4:\text{Tb}^{3+}$ at ($x = 0.286, y = 0.477$), (b) $\text{CaAl}_2\text{O}_4:\text{Eu}^{3+}$ at ($x = 0.637, y = 0.360$) and (c) $\text{CaAl}_2\text{O}_4:\text{Tb}^{3+};\text{Eu}^{3+}$ at ($x = 0.354, y = 0.337$).

4. Conclusion

In conclusion, a new potential white light emitting $\text{CaAl}_2\text{O}_4:\text{Tb}^{3+};\text{Eu}^{3+}$ nanophosphor was synthesized using the combustion method. The structure of the phosphors is consistent with standard monoclinic CaAl_2O_4 . The SEM images confirm the irregular particle shape that was produced from the combustion reaction. The estimated band gap energy agrees with the other measured values. Furthermore, PL excitation spectrum confirmed that the excitation through absorption of the $4f \rightarrow 5d$ transitions of Tb^{3+} and charge transfer transitions of $\text{O}^{2-} \rightarrow \text{Eu}^{3+}$ which agreed with different studies. Finally, the white light occurred after excitation by photons of sufficiently high energy which come from $4f \rightarrow 5d$ transitions of Tb^{3+} and $\text{O}^{2-} \rightarrow \text{Eu}^{3+}$.

Acknowledgement

The authors send gratitude to the National Research Foundation (NRF) for funding the project and the Cluster program of the University of the Free State and the microscopy department at the University of the Free State.

References

- [1] Mothudi BM, Ntwaeaborwa OM., Pitale SS and Swart HC 2010 *Journal of Alloys and Compounds* **508** 262.
- [2] Eeckhout KV, Philippe FS and Poelman D 2010 *Materials* **3** 2536.
- [3] Shaat S K K, Hendrik S C and Odireleng MN 2012 *Optical Materials Express* **2** 962.
- [4] Rivas Mercury JM., De Aza AH and Pena P 2005 *Journal of the European Ceramic Society* **25** 3269.
- [5] Kunimoto T, Kakehi K, Yoshimatsu R, Honda S, Ohmi K and Tanaka S 2002 *Uvsvor Act Rep* **2001** 116.
- [6] Bohdan P, Marek G, Benedykt K, Yuriy O, Oleksandr S, Dmitriy K and Andrew P 2010 *Optica Applicata* **2** 413.
- [7] Bo L, Chaoshu S and Zeming Q 2005 *Applied Physics Letters* **86** 191111.
- [8] Martínez-Martínez R, Álvarez E, Spanghini A, Falcony C and Caldiño U 2010 *Materials Research Society* **25(3)** 484.
- [9] Wang D, Yang P, Cheng Z, Wang W, Hou Z, Dai Y, Li C and Lin J. 2012 *Journal of Colloid and Interface Science* **365** 320.
- [10] Stanislava J, Linda S, Guillaume R, Yaroslav F, Damien B, Philippe B 2007 *Journal of Physics and Chemistry of Solids* **68** 1147.
- [11] Grobelna and Bojarski 2009 *Journal of Non-Crystalline Solids* **355** 2309.
- [12] Fan S, Yu C, He D, Wang X and Hu L 2012 *Optical Materials Express* **26** 765.